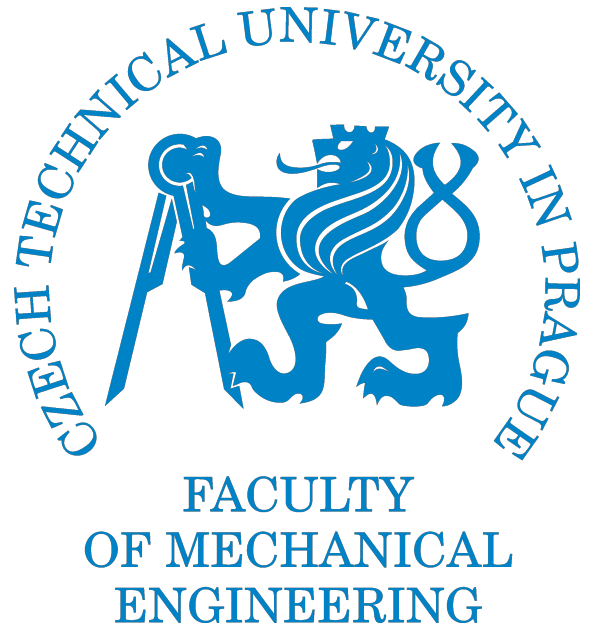

DEPARTMENT OF INFORMATION AND
AUTOMATION TECHNOLOGY

The impact of outer surface roughness to the performance of a small rocket with D class engine

BACHELOR THESIS

Supervisor: Ing. Mgr. Daniel Hadraba, Ph.D.

Prague, 2023

Santiago Müller

Declaration

I declare that I have worked on this thesis independently assuming that the results of the thesis can also be used as the discretion of the supervisor of the thesis as its co-author. I also agree with the potential publication of the results of the thesis or of its substantial part, provided I will be listed as the co-author.

Prague …… ……

Signature

Acknowledgement

I would like to express my deepest gratitude to my thesis advisor, Ing. Mgr. Daniel Hadraba, Ph.D., for his invaluable guidance, support, and encouragement throughout my research journey. His insightful comments, constructive feedback, and constant motivation were instrumental in shaping this thesis and helping me develop my analytical and critical thinking skills.

I would also like to thank the faculty and staff of CVUT, who provided me with a stimulating academic environment and access to the necessary resources for my research. Their dedication and professionalism were truly inspiring and made this thesis possible.

Finally, I want to extend my heartfelt thanks to my family and friends, who have always been there for me, offering their unwavering love, support, and encouragement. Their understanding and patience have been essential in helping me balance my academic pursuits with my personal life.

Thank you all for your invaluable contributions to my academic and personal growth.

Abstract

The impact of outer surface roughness on the performance of small rockets with D class engines was investigated in this study. The goal was to determine how roughness affects the aerodynamics of small rockets and its impact on their overall performance. The study used various surface roughness parameters, The Arithmetic Average Roughness (Ra) and maximum height deviation, to quantify the roughness of the outer surface of the rocket. The results showed that there was a significant relationship between roughness and drag, with roughness having a negative impact on the rocket's aerodynamic performance. The results of this study have implications for the design and production of small rockets, as they suggest that reducing outer surface roughness can lead to improved performance and stability. This study contributes to the growing body of research on the impact of surface roughness on the performance of small rockets and will be valuable for engineers and designers working in this field.

Table of Contents

Figure list

1 Introduction

The design and performance of small rockets have been a focus of research in recent years, with a particular emphasis on their aerodynamics and stability which are strongly related of surface quality and roughness. Surface roughness is influenced by various factors, including manufacturing processes, material properties or environmental conditions, and it has a significant impact on the drag and performance of small rockets. The goal of this study was to investigate the relationship between surface roughness and the performance of small rockets with D class engines. By exploring this relationship, the study aims to provide insights into the impact of surface roughness on small rockets which is crucial for decision making process of hobby or professional designers. This introduction provides a background on the significance of this research and sets the stage for the results and conclusions that will be presented in the study. In addition to that, the data can be used by Y-team under U12113 for optimizing the rocket that participates annually in Czech Rocket Challenge.

2 Surface Roughness

Surface roughness refers to the irregularities or variations in the surface texture of an object. It is often measured by the height, depth, and frequency of the surface irregularities. Roughness can occur naturally, such as in rocks or wood, or it can be intentionally added to surfaces for functional or aesthetic purposes [1].

Surface roughness can be caused by various factors, such as the manufacturing process, material properties, environmental conditions, and wear and tear. It can also be intentional or unintentional, depending on the specific application and requirements [2]. Surface roughness is an important property of materials and surfaces that can significantly impact their behavior and performance in various applications. In the field of mechanical engineering, surface roughness can affect the friction, wear, and durability of machine components, such as bearings, gears, and pistons. Surface roughness can also impact the efficiency and performance of engines and other mechanical systems. In the field of materials science, surface roughness can be a critical factor in optimizing the properties of materials for specific applications, such as increasing the adhesion of coatings or improving the biocompatibility of implants. Surface roughness can also be

an important property in the study of biological systems, as it can affect the adhesion and interactions of cells and tissues.

The classification of surface roughness using parameters is unfortunately not enough for us to fully describe the shape of the surface, but it provides the basic assumptions of the component's function during operation. If we use standardized parameters, we can achieve a clearly defined measurement. Quantitative measurement of the roughness of functional surfaces serves us to increase the quality, efficiency, service life, and above all the reliability of the product. I can say from my own experience that some companies still use this marking today. It depends on the designer's experience which of the parameters are suitable for measurement and their evaluation in relation to the required function of the surface of the part. Due to the performance of today's devices, the number of evaluated parameters is often not limited. Evaluation of surface roughness is precisely characterized in ISO 4287. This standard establishes names and definitions. The height, longitudinal and shape characteristics of the surface are described in this standard. The cited standard defines 9 height characteristics, 1 roughness parameter in the longitudinal direction and 5 shape characteristics.

Overall, surface roughness is an important parameter to consider in a wide range of fields and applications, and understanding its effects can lead to improved performance and functionality of materials and systems. Therefore, the study of surface roughness can be an essential aspect of research in various fields, and it can be crucial to explore its behavior and optimization for different applications [3, 4, 5, 6, 7].

2.1.1 Overview and Analysis of Standards

The structure of the surface, the definition of the parameters and suitable measurement methods are part of the standards GPS (Geometrical Product Specifications), on which this bachelor's thesis is based. The content of the standards is discussed in more detail in the following chapter. The part describing the standard ISO 4287 is not only a description of the surface roughness, but also of the waviness and the basic profile, which is related to the surface roughness. Surface roughness is only one part of the surface properties.

2.1.1.1 Geometrical Product Specifications (GPS) – Surface structure: Profile method – Terms, definitions and parameters of surface structure ISO 4287 – 1997

The standard ISO 4287 defines names, terms, parameters and definitions in the field of integrity surface such as roughness, waviness and primary profile obtained by the profile method. It relies on the knowledge of the λS, λC and λf filters addressed on chapters 2.1.2.5, 2.1.2.6 and 2.1.2.7. It lists the roughness profile and its parameters as its own defined feature of the surface structure. It leaves a periodic and random profile to the subjective opinion of the user. The current standard defines 2D features, and in the future 3D features will be included for three-dimensional evaluation of the surface. ISO 4287 was adopted on January 26, 1998.

2.1.1.2 Geometrical Product Specifications (GPS) – Surface structure: Profile method – Rules and procedures for assessing surface structure ISO 4288 – 1996

The ISO 4288 standard is a general GPS standard (Geometrical Product Specifications). The standard establishes rules for comparing values with the tolerance limits established for surface parameters. It also specifies the rules for selecting cut-off wavelengths λC for surface roughness parameters measured with ISO 3274 probes. This standard replaces the original first edition from 1985. The main difference is the selection of the cut-off wavelengths. Now the values are selected according to the surface structure of the work piece and not according to the information in the drawing. This standard describes the evaluation of roughness profile parameters and basic profile parameters. This standard was adopted on November 2, 1997 [8].

2.1.2 Concepts of parameters

We distinguish two types of basic geometric irregularities: macro-geometry and micro-geometry. The shape deviations and waviness are listed as macro-geometric parameters (macro-irregularities) and micro-geometry contains surface roughness (micro-irregularities). When measuring roughness, we must ensure that the effects of waviness are not reflected in the measured values and shape deviations. This is achieved by choosing the right basic length, thanks to which other factors not related to surface roughness are largely filtered out. The distance between the highest and the lowest waviness protrusion is greater than the roughness. In addition, we need to choose a greater length of the measuring section for the measurement of waves [9].

2.1.2.1 Primary Profile

It is the basis for the evaluation of the primary profile parameter. The p-parameter is geometric parameter calculated from the base profile. Illustrated in Figure 1 b) [8].

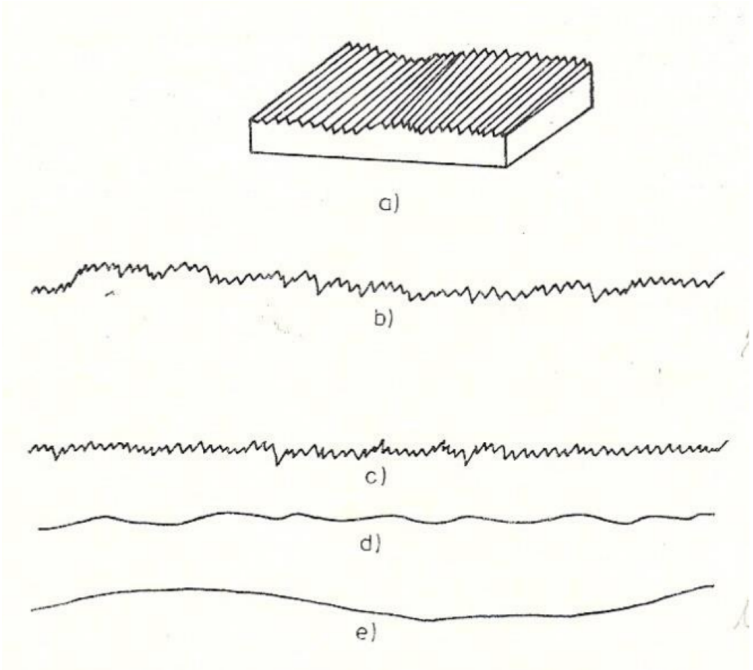

Figure 1 – Profiles – a) b) c) d) e) the deviation of the surface shape. Copied from [10].

2.1.2.2 Roughness profile

It is created by deriving from the primary profile by suppressing the long-wave components in use profile filter λc to λs. The R-parameter is calculated from the roughness profile. An example is in the Figure 1 c) [8].

2.1.2.3 Waviness profile

This profile is created when a filter with a value of λf suppressing long-wave components and λc is reached suppressing short-wave components. We calculate the W-parameter from the waviness profile. For waviness we consider larger irregularities than roughness. On the waviness is superimposed (layered) roughness. Figure 1 d) shows the waviness profile [8].

We will use this knowledge of geometric parameters to determine the type of evaluation parameter profile. For example, the Ra parameter is calculated from the roughness profile and the parameter Pt is calculated from the primary profile. In practice, the distribution of roughness,

waviness and shape deviations is taken with respect to size component – surface. The pitch of the bumps has an effect to the resulting inequality classification. For example, the unevenness of the shape of a small shaft, which was defined as a shape deviation, it can be of the same size with a larger number of such unevenness of the large shaft is taken as waviness [8].

2.1.2.4 Profile filter

The profile filter is a basic element for measuring parameters divides the profile into long-wavelength and shortwave components. According to ISO 11562, there are three filters defined. The profile filters have the same transmission characteristics (Figure 2), but the values of the cut-off wavelengths are different. We can encounter the textual equivalent λS = Ls etc. [8].

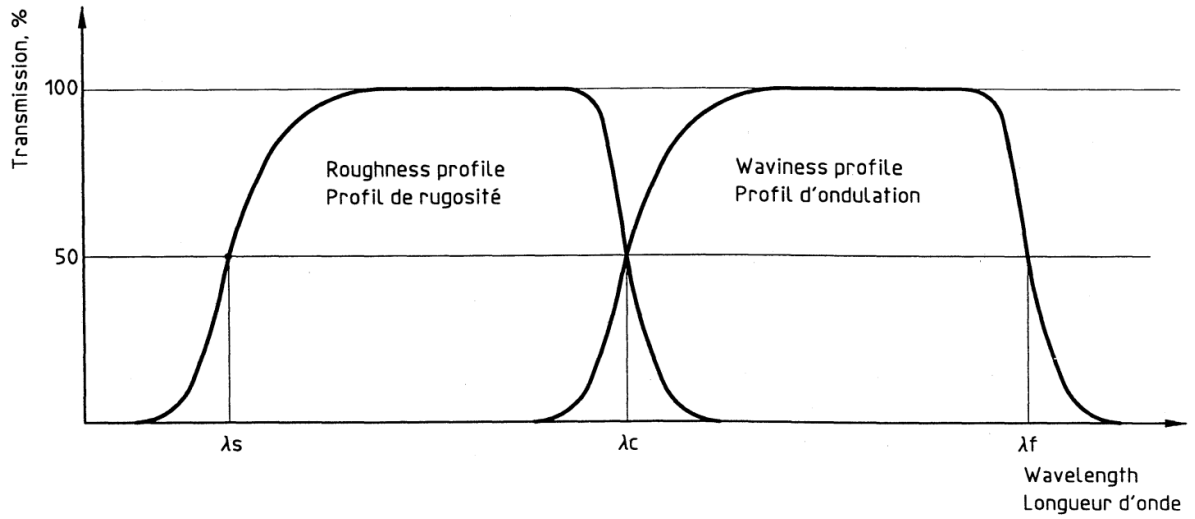

Figure 2 – Transmission characteristic of roughness and waviness profiles copied from [8]

2.1.2.5 λS filter profile

This filter defines the difference between the roughness and smaller components of the surface roughness [8].

2.1.2.6 λC filter profile

Defines the interface between roughness and waviness componets [8].

2.1.2.7 λf filter profile

This filter divides the interval between waviness and longer components of surface defects [8].

2.1.2.8 Coordinate System

The coordinate system defines the parameters of the surface structure. It is used here rectangular coordinate system with a right-handed Cartesian system, where the X-axis is parallel to the center line, the Y-axis is in the direction of the actual surface and the Z-axis is defines the space between the surface and the surroundings, see figure 3. The profile of the surface is created by interposing surfaces in the XZ axes [8].

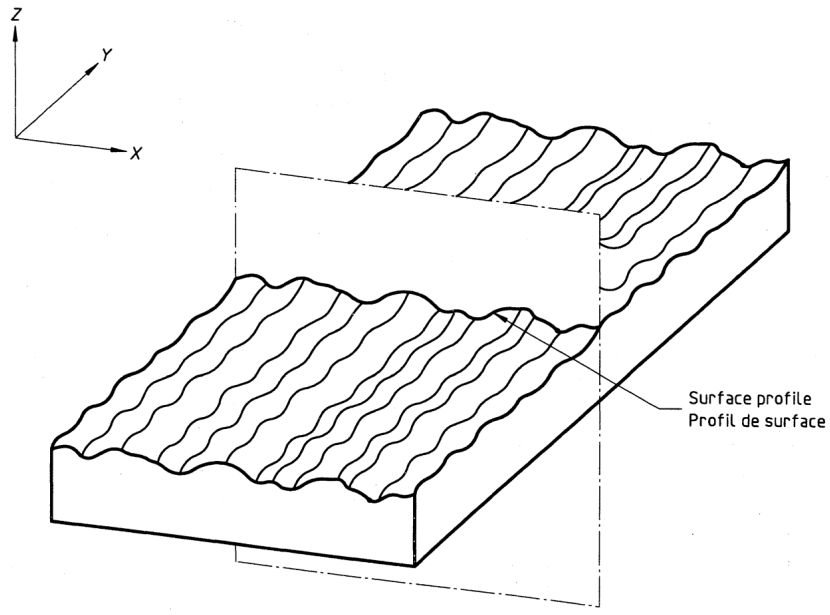

Figure 3 - Coordinate System copied from [8]

2.1.2.9 Geometric nominal surface

Geometric nominal surface is defined as a surface with perfect properties and its shape is determined by technical documentation, for example a drawing [11]. Such surface is unrealistic. In the resulting product, we encounter a real surface bordering the manufactured part with certain surface imperfections.

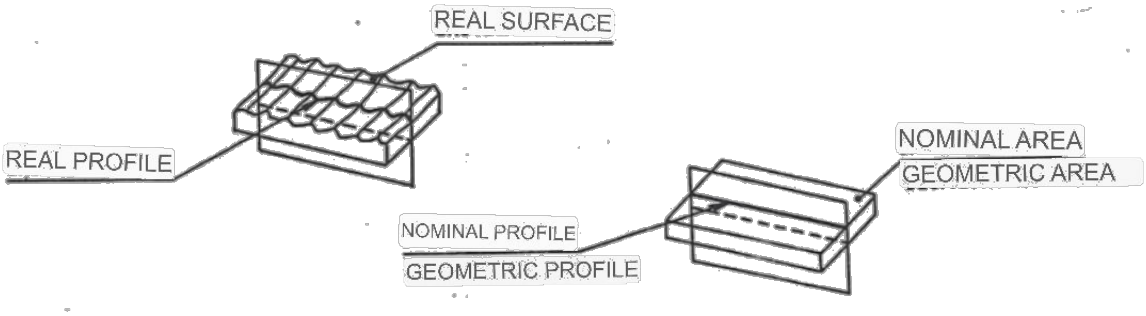

Figure 4 - Actual and nominal profile - copied and translated from [11]

2.1.2.10 Real surface

The real surface is the area formed by the boundary between the body and the environment. The character of the roughness may differ in individual measurement directions. A real surface contains irregularities of varying degrees and sizes. The real surface is formed by a combination of roughness, waviness and shape deviations [11].

2.1.2.11 Cross profile

This profile is created if we cut the surface with a plane perpendicular to the direction of the surface roughness. An example is in Figure 8 [11].

2.1.2.12 Longitudinal profile

A longitudinal profile is created if we use a plane in the direction of the unevenness of the examined profile. It means that the inequalities must have a predominant direction of occurrence [11].

Figure 5 - Transverse and longitudinal profile - copied and translated from [11]

2.1.2.13 Basic length *l*

The basic length is used to assess inequalities in the evaluated length, which is in the coordinate system in the direction of the X axis. The base lengths should have the same dimension. The base length should be long enough to respect the roughness measurement and at the same time reasonably short in order to exclude the detection of larger geometric deviations – waviness. [8] This filtering can be done mechanically, determined by the parameters of the sensor, where the largest the radius of rounding of the sensing tip, the radius of rounding of the support foot has an effect and the distance between the sensing tip and the support foot. This configuration ensures that the sensor acts as a filter in itself. In the case of the profilometer, an electric filter is used to the fundamental length given by the wavelength. Digital filtering, often used today, is possible with the help of software that uses discrete Fourier transforms. Using different short-pass, long-bass and band-pass filter levels, we can filter out individual profile irregularities and investigate them further [10].

Digital filters are not physically limited, and filtering is possible according to any setting basic length. To ensure similar results, it is necessary to perform filtering according to standard of basic lengths. A selection of suitable basic lengths includes standard ISO 4288 [10].

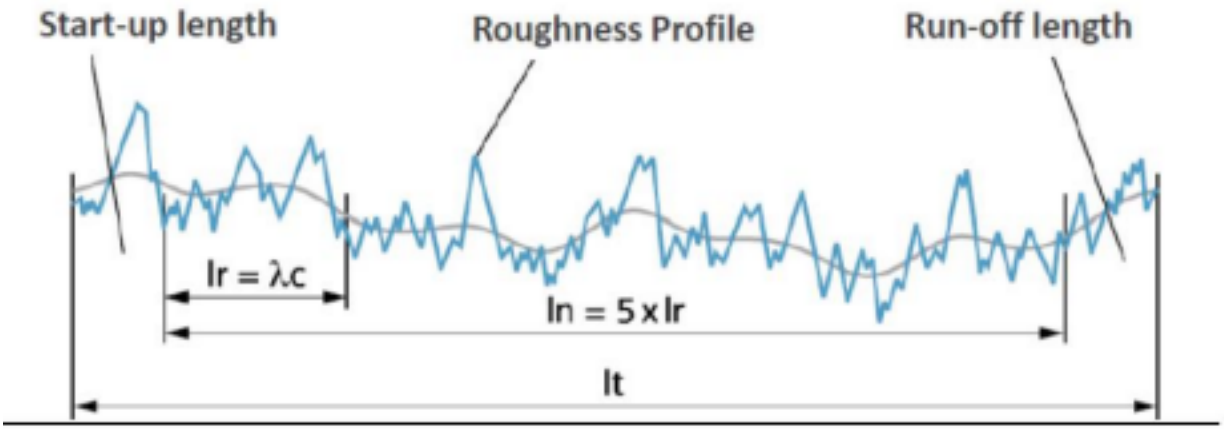

Figure 6 - Basic length – Coped from [12].

The dimension of the basic length and the subsequent corresponding evaluated length are chosen according to the estimation of the dimension of the measured parameter, according to the table from the standards [8] for periodic and non-periodic profiles. They are mostly chosen from

lengths: 0.08, 0.25, 0.8, 2.5 and 8.25 mm. Apart from the parameters R_t and R_{mr}, all roughness parameters are related to the base length.

2.1.2.14 Evaluated length l_n

This length determines the dimension on which we evaluate the examined roughness. The evaluated length contains one or more basic lengths. Evaluated the length ln is equal to the length of the base length for the base profile $\boldsymbol{l_p}$ and is in the coordinate system in the direction of the X axis [11].

Equation 1 tells about the ratio of the evaluated length to the basic length.

$$l_n = \sum_{i=1}^{i=m} l_i \tag{1}$$

2.1.2.15 The length of the measured section l_t

This length is used to evaluate the roughness profile. Length contains one or more basic lengths, plus the distance for the start and finish of the measurement, which they exclude mechanical and electrical measurement instabilities [11].

2.1.2.16 Profile deviation y

Profile deviation is the perpendicular distance between the measured surface and the base line [2].

2.1.2.17 The mean line of the least squares of the profile - mean line - m

This base line is created by dividing the real profile in the range of the base length, by the sum of the squares of the deviations of the profile so that the sum on both sides is as small as possible (Equation 2).

$$\int_0^l y^2 dx = min \tag{2}$$

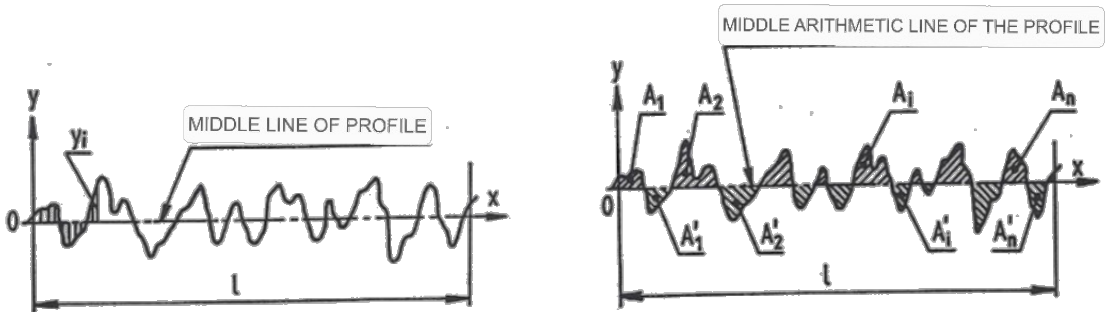

Figure 7 - Mean (arithmetic) profile line – copied and translated from [11]

2.1.2.18 Maximum profile peak height Rp (ISO 4287)

This parameter is determined by the highest element of the profile protrusion in the range of the basic length l. The parameter Rp is determined by the length from the center line with the highest point of the measured profile, as it is shown in Figure 9 [8].

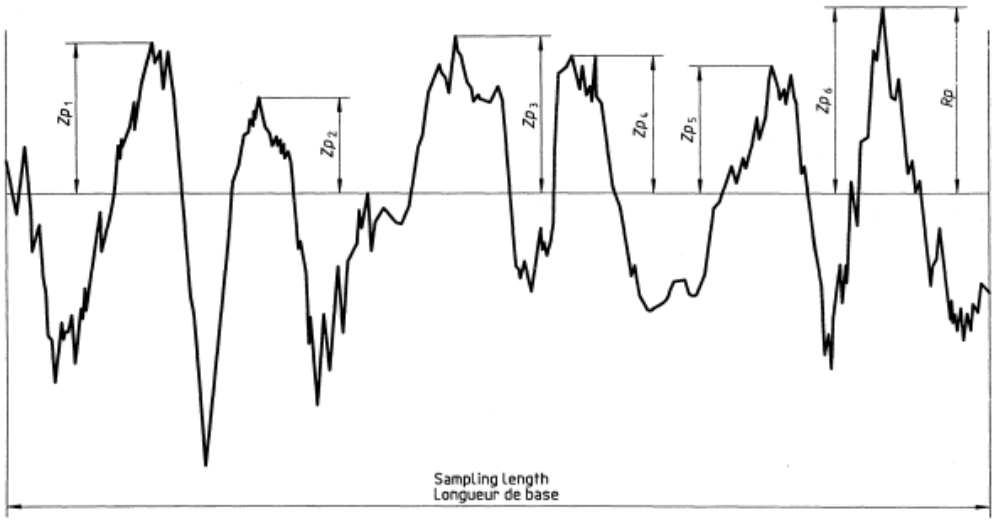

Figure 8 - Rp - copied from [8]

2.1.2.19 Maximum profile valley depth Rv (ISO 4287)

The parameter Rv is determined by the distance between the center line and the lowest point of the depression of the actual surface marked as Zv on the base length. Illustrated in Figure 10 [8].

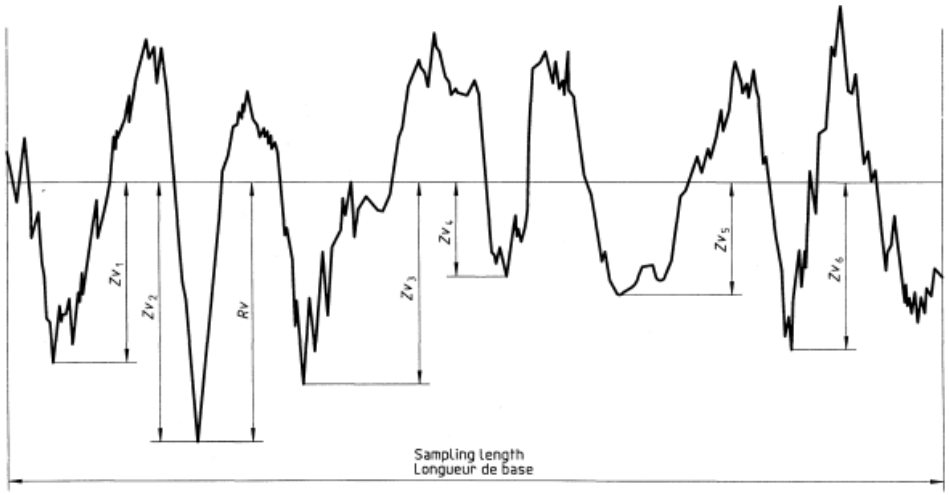

Figure 9 – Rv - copied from [8]

2.1.2.20 Maximum height of profile Rz

This height characteristic Rz is defined as the sum between the line of the highest peak Rp and the line of the lowest groove of the profile Rv in the range of the basic length l. It only indicates the largest difference in the unevenness of the measured surface in the interval of the basic length. For the functional properties of the surface, this parameter is of little importance, it is used as a supplementary parameter to represent the roughness. One deeper groove will strongly affect the result of an otherwise smooth ground surface. Multiple measurements are appropriate here [8].

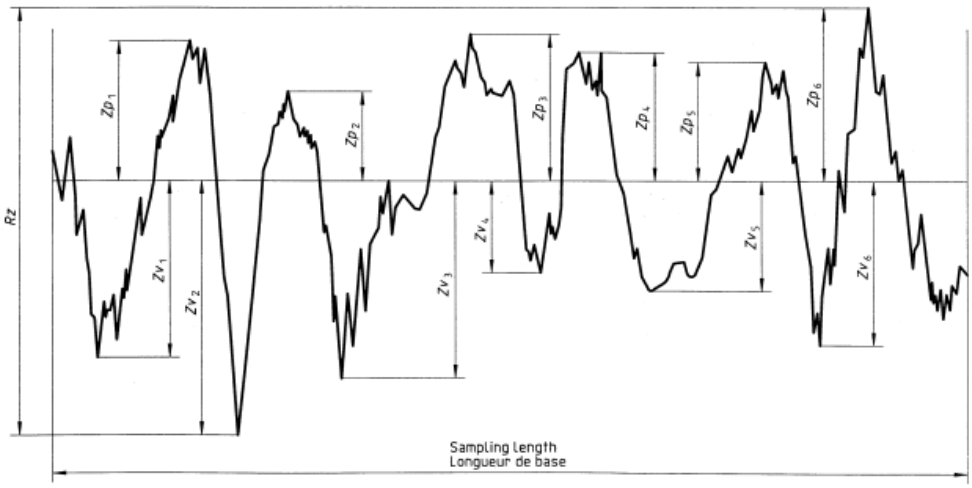

Figure 10 – Rz - copied from [8]

$$R_z = R_p + R_v \tag{3}$$

2.1.2.21 Total profile height Rt (ISO 4287)

This parameter is determined by the sum of the highest projection Rp and the lowest depth Rv in the range of the evaluated length. Given the knowledge of the difference between the basic and the evaluated length (Equation 4) [8].

$$R_t \geq R_z \tag{4}$$

It is evident that the parameter Rt is not determined by the center line and its value is affected by grooves, defects and impurities of the surface. The total profile height *Rt* frequently equals to maximum height profile *Rz*.

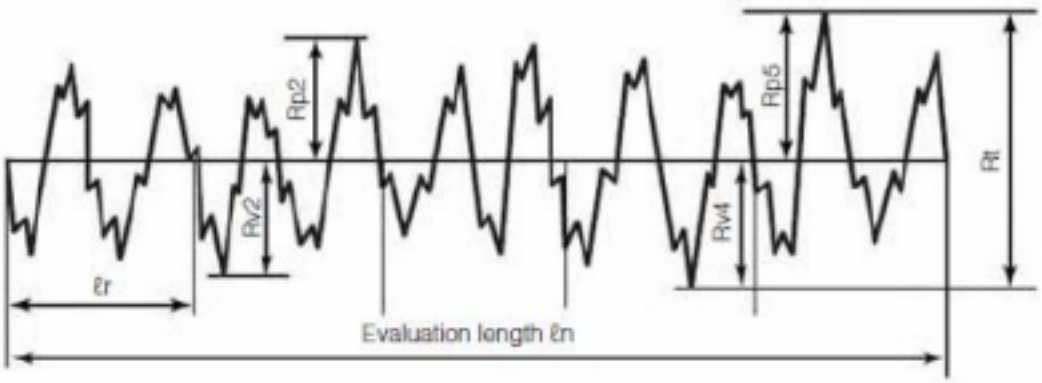

Figure 11 – Rt - copied from [8]

2.1.2.22 Average height of profile elements Rc (ISO 4287)

Average height of profile elements Rc is represented by the arithmetic average of the Zt heights over the base length range. Rc is defined by the height of the profile element Zt as the sum of absolute values of peak height and trough depth, which is then divided by the number these elements as derived from Figure 13 and demonstrated in Equation 6 [8].

$$R_c = \frac{1}{m}\sum_{i=1}^{m} Zt_i \tag{6}$$

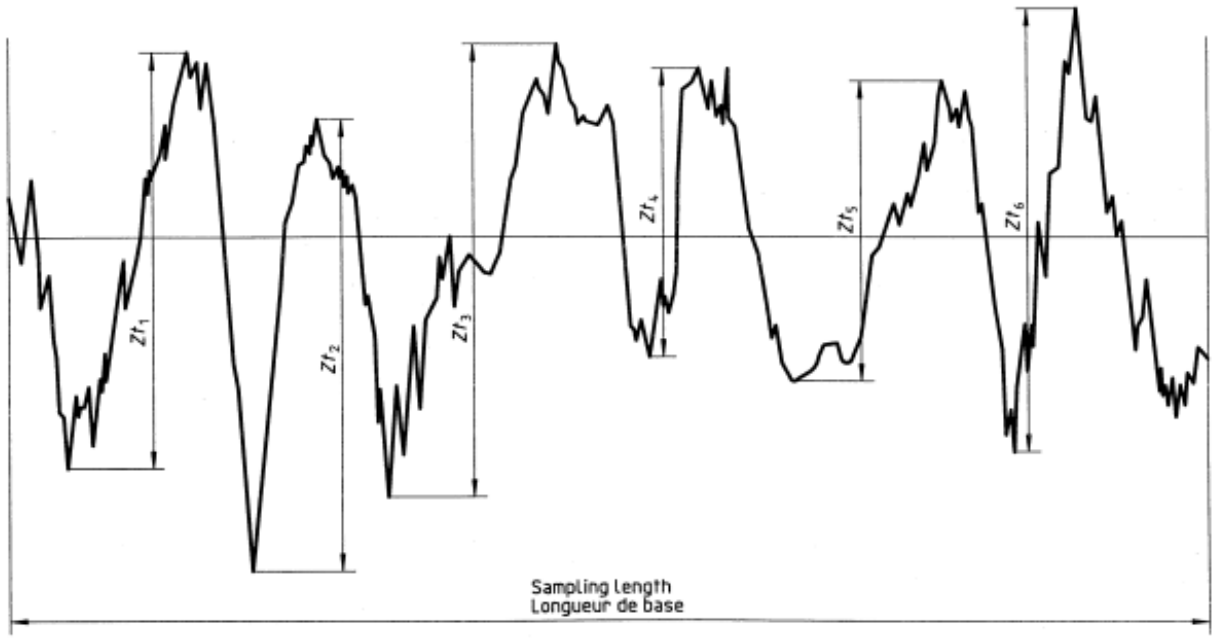

Figure 12 – Rc - copied from [8].

2.1.2.23 Mean square deviation of roughness Rq (ISO 4287)

Rq is the root mean square value of the roughness profile deviations from the mean line over the evaluation length [1]. It provides a measure of the average height deviation from the mean line in a surface profile. Rq considers the absolute values of all the surface deviations, not just the peaks and valleys. It is calculated by taking the square root of the sum of the squares of the height deviations, divided by the evaluation length (Equation 7) [8, 11].

$$Rq = \sqrt{\frac{1}{l}\int_0^l z^2(x)dx} \tag{7}$$

where, l is the evaluation length, z is height and x is the distance along measurement.

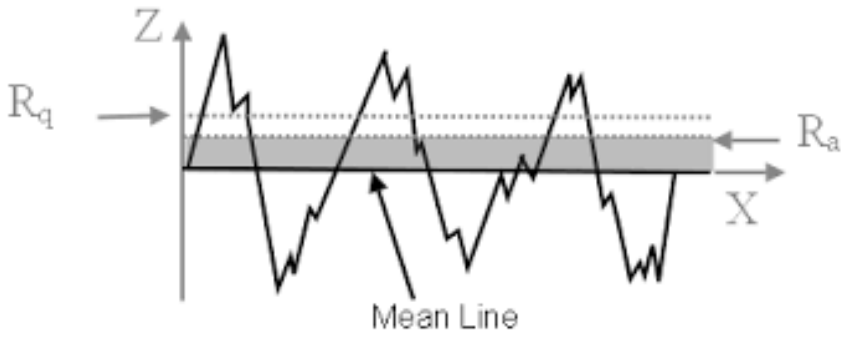

Figure 13 – Rq - copied from [8]

2.1.2.24 Arithmetical mean deviation of the assessed profile Ra (ISO 4287)

The mean arithmetic deviation of the profile is a surface parameter widely used in the Czech Republic. This standard is probably popular for its simplicity of measurement and accuracy of repeated measurements. Ra as a height parameter identifies the mean value of the distances from the center line, in other words, it is the arithmetic mean of the absolute deviations of the filtered roughness profile from the center line on the measured range of the basic length l.

This characteristic is displayed by the height of a rectangle constructed on the center line with the same content as the profile unevenness bounded profile and midline. This purely statistical value has a very low ability to talk about the actual roughness of the surface. It is caused by neglecting the distinction between extreme protrusions and depressions, so two different surface shapes can return the same Ra value, however the surfaces will act differently and one of the surfaces can develop cracks much faster. The recommendation of the standards to measure the surface at least on five basic lengths and to average the results yields more representative results. The correct assessment of the value of the Ra parameter is only possible with the correct selection and indication of the basic length. For the static assessment of roughness, the root mean square deviation of the roughness has a better indicative value [8, 11].

$$Ra = \frac{1}{l}\int_0^l |z(x) - z_c| dx \tag{8}$$

Where l is the evaluation length, $z(x)$ is the height of the surface profile at given point x, and z_c is the position of the center line.

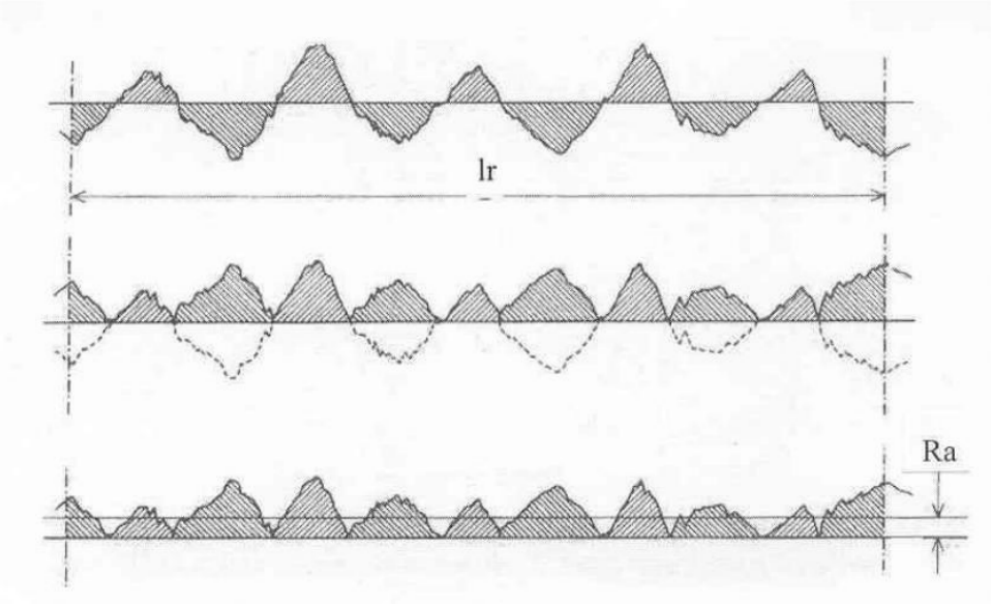

Figure 14 - Graphic interpretation of Ra - copied from [13]

2.2 Roughness & Drag relationship

Surface roughness is one of the key factors in the aerodynamic drag of various applications, such as aircraft, automobiles, ships, and wind turbines. The relationship between surface roughness and drag is important to understand in order to optimize the performance, efficiency, and safety of these systems [14, 15]. Experimental and theoretical studies have shown that rougher surfaces experience more drag than smoother surfaces, due to the increased friction and turbulence caused by the surface irregularities. The amount of drag can be quantified by the drag coefficient(C_d), which is defined as the ratio of the drag force (F_d) to the product of the dynamic pressure (q) and the reference area (A) described in Equation 9 [16].

$$C_d = \frac{2F_d}{qA} \tag{9}$$

To predict and control the drag coefficient, various models and methods have been developed based on the specific flow conditions, surface properties, and geometry. The Reynolds-

averaged Navier-Stokes (RANS) equations, boundary layer theory, Nikuradse correlation, and Colebrook-White equation are some commonly used models [17, 18]. However, the relationship between surface roughness and drag is complex and depends on multiple factors, such as the flow velocity, viscosity, temperature, surface material and roughness distribution. Therefore, experimental validation and numerical simulation are often necessary to accurately predict and optimize the drag performance of a given system [19, 20].

The major problem is that the roughness elements such as bumps, seams, and imperfections on the surface of a rocket cause flow separation and increase of drag. The relationship between surface roughness and drag is important to understand in order to optimize the performance and stability of the rocket during flight [21, 22]. Experimental studies have shown that surface roughness can increase drag by up to 10% in model rockets [23]. This effect is more pronounced at lower Reynolds numbers, which are typically encountered during the ascent phase of the rocket's flight. The drag coefficient of a model rocket can be estimated using empirical formulas such as the Schlichting formula [24], which considers the Reynolds number, surface roughness height, and shape of the rocket see Equation 10 [25].

$$D = Cd\frac{\rho V^2}{2}A \tag{10}$$

Figure 15 - Rocket Aerodynamic forces copied from [26]

2.3 Ways to measure roughness

Contact profilometry is one of the most widely used methods for measuring surface roughness. It involves scanning a stylus across the surface and recording its vertical displacement. This method is accurate and reliable but may damage delicate surfaces [27].

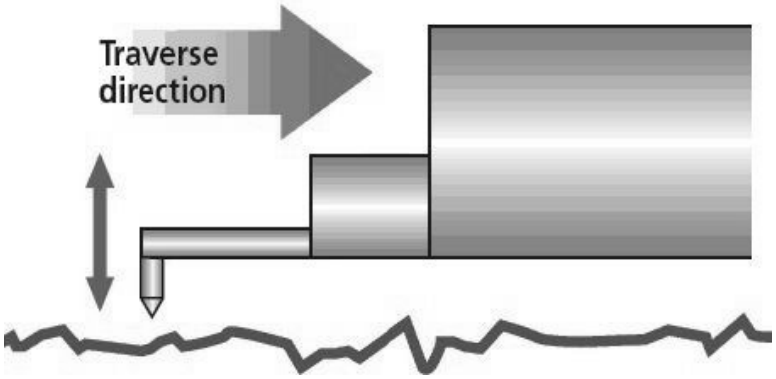

Figure 16 - Contact Profilometry - copied from [27]

Atomic force microscopy (AFM) is a high-resolution imaging technique that uses a cantilever with a sharp tip to scan the surface of a sample. As the tip moves across the surface, it measures the force between the tip and the surface. This method provides high-resolution images of the surface but can be time-consuming [28].

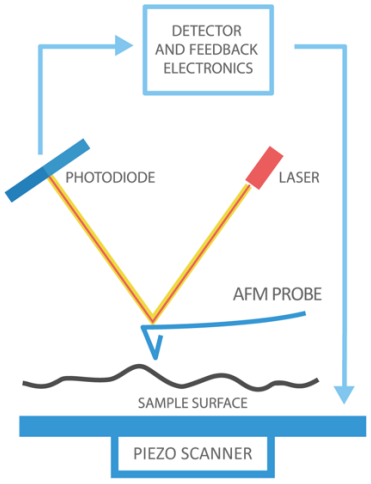

Figure 17 - Atomic force microscopy - copied from [32]

Scanning electron microscopy (SEM) is another technique used to visualize the surface of a sample at high magnification. The electron beam scans the surface of the sample, and the

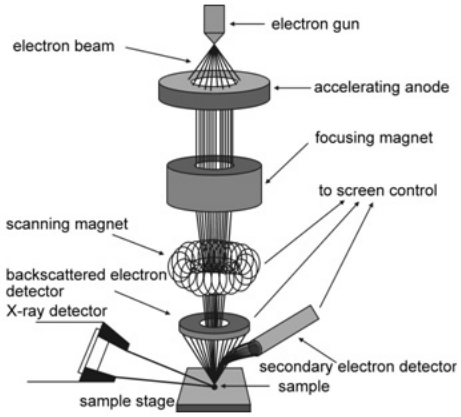

electrons scattered or emitted from the surface are collected and used to create an image of the surface. This method provides high resolution images of the surface, but the sample must be prepared and coated with a conductive material [29].

Figure 18 - Scanning electron microscopy - copied from [33]

Confocal microscopy is a powerful nondestructive method in which a confocal microscope scans the surface of a sample and produces a three-dimensional image of the surface. The microscope scans the surface with a laser and collects light reflected or emitted from the surface. This method provides high-resolution images of the surface and has the added benefit of revealing features below the surface. Confocal microscopy is widely used in biotechnology and materials science to study surface roughness and its effects on the physical and biological properties of materials [29, 30, 31].

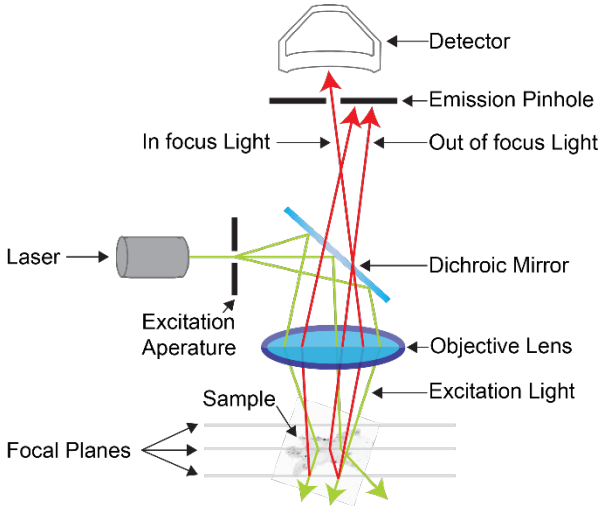

Figure 19 - Confocal microscopy - copied from [31]

To achieve high-quality surface imaging with confocal microscopy, it is important to choose the appropriate objective lens and to optimize the laser scanning parameters. Various confocal microscopy techniques have been developed to improve the imaging capabilities of the instrument, including multiphoton microscopy and super-resolution microscopy, however, this method is still diffraction limited and its xy, z resolution is approximately 200 nm, 400 nm respectively[70]. Additionally, image processing and analysis tools are used to extract quantitative data from confocal microscopy images, such as surface roughness parameters like *Ra*, *Rq*, and *Rz* [30, 31].

2.4 Ways to decrease roughness

Polishing is a widely used method for decreasing surface roughness. The mechanical polishing process involves using abrasive material to remove surface irregularities and create a smoother surface [34]. The chemical polishing process involves using a chemical solution to dissolve the surface layer, creating a smoother surface. Chemical polishing is usually preferred for materials that are difficult to polish mechanically, such as ceramics and glasses [35].

Coating the surface with a thin layer of material is another method to reduce surface roughness. The coating material is usually chosen for its ability to fill in surface irregularities and create a smoother surface [36]. In contrary, one can selectively remove the material from the surface as when performing chemical etching. Chemical etching is a process that involves specific chemical treatment of the surface to dissolve the material and produce the surface smoother [37, 38]. There are other methods such as electropolishing, plasma treatment, laser surface modification or acetone vapor polishing.

Electropolishing is an electrochemical process that can be used to smooth and polish metal surfaces. It involves immersing the metal in an electrolyte solution and passing an electric current through it. The process dissolves the surface irregularities and leaves a smoother surface [39]. Plasma treatment is a non-thermal process that can modify the surface of a material. The process involves exposing the material to a plasma, which can remove surface contaminants and modify surface roughness. The plasma treatment can be performed under different conditions to obtain the desired surface roughness [40]. Laser surface modification is a process that involves using a laser to modify the surface of a material. The laser beam can selectively remove material from the surface, resulting in a smoother surface [41]. Acetone vapor polishing is a post-processing technique used to smooth out the surface of 3D-printed parts made from certain types of plastics, such as ABS or ASA. The process involves exposing the 3D-printed part to acetone vapor, which causes the surface of the part to melt and reflow, resulting in a smooth and glossy finish [48]. This was the method that was used in this bachelor's thesis, and it will be addressed in more detail in chapter 2.5.

2.5 Acetone vapor polishing

Acetone vapor polishing is an effective technique for achieving a smooth finish on 3D printed objects and has been used in various industries, including automotive, aerospace, and medical device manufacturing. It is a cost-effective alternative to traditional finishing techniques, such as sanding and painting, and can be performed on objects of varying shapes and sizes [49]. When exposed to acetone vapor, the plastic material on the surface of the 3D printed object begins to soften and dissolve slightly. This is due to the ability of acetone to break down and dissolve the polymer chains that make up the plastic material. Specifically, acetone acts as a solvent for the plastic, causing the surface to become sticky and pliable [48]. As the acetone penetrates the surface of the object, it also melts the plastic and causes it to flow again, smoothing out imperfections or layer lines. The heat generated by the reaction also helps to further dissolve the plastic material, making the surface even smoother [48]. The duration of exposure to acetone steam is an important factor in achieving the desired surface quality of the object. If the object is exposed to the steam for too long, the plastic material may become too soft and deform or lose its structural integrity. On the other hand, if the object is not exposed to steam long enough, the surface may not become completely smooth [50]. It is important to note that not all types of plastics can be polished with acetone vapor. In general, only plastics that are soluble in acetone, such as ABS and ASA, can be polished using this technique. Other plastics, such as PLA, are not soluble in acetone and may not be affected by the vapor [50]. The process is relatively simple and requires only a few items: a container with an airtight lid, a small amount of acetone, a platform to hold the object, and the object itself. The object is placed on the platform, which is then placed inside the container. A small amount of acetone is added to the container, and the lid is sealed, creating an airtight environment. The acetone vaporizes and begins to penetrate the surface of the object, smoothing out any roughness or layer lines. The length of exposure time can vary depending on the size of the object and the desired level of finish, but typically ranges from a few minutes to several hours. However, it should be noted that acetone is a highly flammable and volatile substance and proper safety precautions should be taken when handling it. The process should be conducted in a well-ventilated area away from ignition sources, and protective equipment such as gloves and a respirator should be worn. In addition, acetone vapors can be harmful if inhaled, and prolonged exposure can cause headaches, dizziness and nausea.

2.6 Additive manufacturing (AM)

Additive Manufacturing (AM), also known as 3D printing, is a manufacturing process that creates a physical object by building it layer-by-layer from a digital 3D model. This technology has been around since the 1980s, but it has recently gained widespread attention due to its ability to create complex geometries, reduce material waste, and enable rapid prototyping and customization [42]. AM has the potential to revolutionize traditional manufacturing processes, as it enables the production of parts with greater precision and complexity than ever before. Instead of subtracting material from a block of raw material, AM adds material layer by layer to create the desired shape. This process allows for the creation of parts with intricate geometries, including hollow and organic shapes that would be difficult or impossible to produce with traditional manufacturing techniques [43]. There are several different AM processes, including Fused Deposition Modeling (FDM), Stereolithography (SLA), Selective Laser Sintering (SLS), and Binder Jetting. Each of these processes has its own advantages and disadvantages, and the choice of process depends on the specific application and requirements of the part being produced [42, 43].

One of the key advantages of AM is its ability to reduce material waste. Traditional manufacturing processes often involve cutting or machining raw material to create the desired shape, which can result in significant amounts of scrap material. In contrast, AM only uses the exact amount of material required to create the part, minimizing waste, and reducing costs [44]. Another advantage of AM is its ability to enable rapid prototyping and customization. With traditional manufacturing processes, creating a prototype can be time-consuming and expensive, as tooling and fixtures need to be created. AM allows for the rapid production of prototypes and can be easily customized to meet specific design requirements [44]. AM is already being used in a wide range of industries, including aerospace, automotive, medical, and consumer goods. In aerospace, AM is being used to create lightweight and complex parts that can improve fuel efficiency and reduce emissions. In the medical industry, AM is being used to create patient-specific implants and prosthetics that can improve patient outcomes [45]. However, there are also some challenges associated with AM.

One of the main challenges is the limited range of materials that can be used in the process. While traditional manufacturing processes can use a wide range of materials, such as metals, plastics, and ceramics, the materials that can be used in AM are currently more limited. This can

be a significant limitation for certain applications, such as those requiring high-temperature resistance or extreme durability [46]. Another challenge is the post-processing required for AM parts. AM parts often require additional processing, such as sanding or polishing, to achieve the desired surface finish. Additionally, some AM processes, such as SLS, require support structures that must be removed after printing, which can be time-consuming and labor-intensive [46]. Despite these challenges, the potential of AM is clear, and it is expected to continue to grow and evolve in the coming years. As more materials become available for use in AM and the technology becomes more refined, the potential for this technology to transform traditional manufacturing processes will only continue to grow [47].

2.7 Types of additive manufacturing – Industrial vs Home

Industrial 3D printing has been in use for several decades and has contributed significantly to various industries such as aerospace, automotive, and healthcare. Home 3D printing, on the other hand, is a relatively new technology that has gained popularity in recent years due to its affordability and accessibility. In this essay, we will discuss the differences between industrial and home 3D printing in terms of their capabilities, applications, and technologies [51]. One of the main differences between industrial and private 3D printing lies in their capabilities. Industrial 3D printing is typically used to produce high-value, complex parts on a large scale. The machines used for industrial 3D printing are often expensive and require specialized training to operate. These machines can produce parts with high accuracy, tolerances, and surface finishes, making them suitable for aerospace, medical implant, and automotive applications [51,52]. 3D printing for home use, on the other hand, is more suitable to produce smaller and less complex parts and objects. Home 3D printers are much cheaper and accessible to individuals, making them ideal for hobbyists, DIY enthusiasts and small businesses. However, parts made with home 3D printers may not have the same accuracy, tolerances, and surface finish as parts made with industrial 3D printers [53]. Industrial and home 3D printing have different applications depending on their capabilities. Industrial 3D printing is used in various industries to produce complex and high-value parts. The aerospace industry, for example, uses 3D printing to produce lightweight and high-strength components for aircraft and spacecraft. The medical industry uses 3D printing to produce custom implants, prosthetics and surgical instruments tailored to the patient's needs. The automotive industry uses 3D printing to manufacture vehicle parts such as engine components, brake calipers,

and dashboard parts [52]. Home 3D printing has several applications, including prototyping, DIY projects, and small-scale manufacturing. Hobbyists use 3D printing to make toys, figurines and other objects that are difficult to find in stores. Small businesses are using 3D printing to create custom products such as cell phone cases, jewelry and home accessories. In addition, home 3D printing is increasingly being used in education to teach students about design, engineering, and manufacturing [53].

Industrial and home 3D printing use different technologies to produce parts and objects. Industrial 3D printing uses a range of techniques such as powder bed fusion, material extrusion, and stereolithography. Powder bed fusion involves the use of a laser or electron beam to melt and fuse metal or plastic powders into a solid form. Material extrusion involves the use of a printer head that deposits material layer-by-layer to create a 3D object. Stereolithography uses a liquid resin that is cured using a UV light to create a solid object [52,53].

Home 3D printing, on the other hand, primarily uses material extrusion techniques, such as fused filament fabrication (FDM) and stereolithography apparatus (SLA). Fused filament fabrication involves the extrusion of molten plastic through a nozzle to create a 3D object. SLA uses a liquid resin that is cured using a UV light to create a solid object. Additionally, home 3D printing may also use binder jetting, which involves the use of a liquid binder that is deposited onto a layer of powder to create a 3D object [53].

In general, industrial 3D printers produce objects with smoother surface roughness than residential 3D printers, due to higher precision and accuracy, larger build volume, and a wider range of materials. However, the specific roughness of an object depends on several factors, such as the type of material used, the build process, and the post-processing techniques used. [54]

The surface roughness achieved by additive manufacturing (3D printing) can vary depending on the technology, material, and printing parameters used. This are some examples of the surface roughness that can be achieved with different 3D printing technologies:

Fused Deposition Modeling (FDM) typically produces parts with a rough surface finish, with roughness values ranging from 20 to 200 micrometers (μm).

Figure 20 - FDM printer ender 3 pro - Copied from [55]

Stereolithography (SLA) produces parts with a smoother surface finish than FDM, with roughness values ranging from 5 to 50 µm.

Figure 21 - SLA printer LH-002R - Copied from [55]

Selective Laser Sintering (SLS) typically produces parts with a rough surface finish like FDM, with roughness values ranging from 50 to 150 µm.

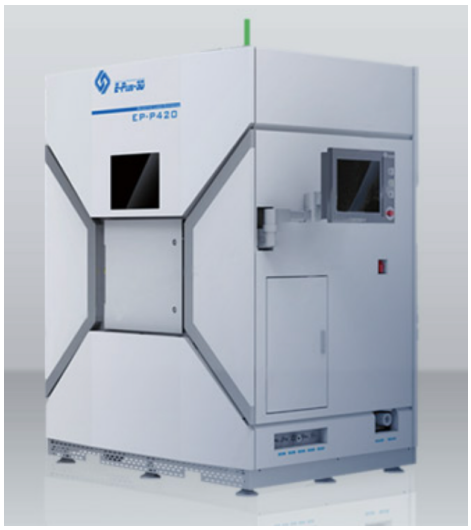

Figure 22 - SLS printer E-Plus-3d - Copied from [56]

Metal Powder Bed Fusion (PBF) can produce parts with a smoother surface finish than FDM and SLS, with roughness values ranging from 5 to 50 µm.

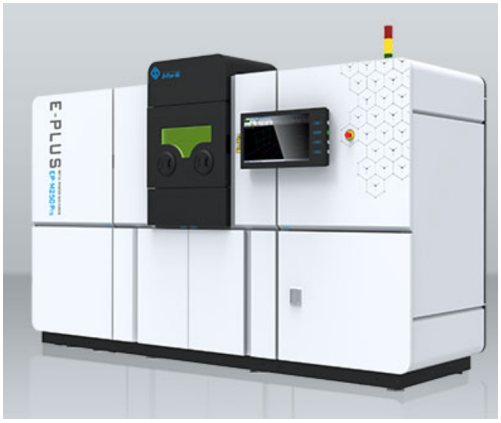

Figure 23 - PBF EP-M250Pro - Copied from [56]

It's important to note that the surface roughness of an object produced by additive manufacturing can be affected by several factors, including the material used, the printing parameters, and the post-processing techniques applied. In many cases, the surface roughness can be improved by post-processing techniques such as sanding, polishing, or electroplating this will be explain in more detail in chapter 1.9.

2.8 Used materials for desktop printers Pro Cons

There are several materials that can be used for desktop printing such as PLA, ASA, Nylon, etc. Polylactic acid (PLA) is a biodegradable thermoplastic widely used in desktop 3D printing. It is made from renewable resources such as corn starch or sugar cane, making it an environmentally friendly material. PLA is also easy to process, as it requires a lower printing temperature and does not produce harmful fumes during printing. In addition, PLA has a high surface quality, making it a popular choice for printing decorative and artistic objects. However, PLA is not as durable as some other materials, as it can be brittle and has lower resistance to heat and UV light [57].

Acrylonitrile styrene acrylate (ASA) is a thermoplastic commonly used in industrial applications but can also be used for desktop 3D printing. It is a strong and durable material that can withstand high temperatures, making it suitable for creating functional parts and prototypes. However, ASA requires a higher printing temperature than PLA and releases toxic fumes during printing, so it must be used in a well-ventilated area or with a special enclosure. In addition, ASA tends to warp and is difficult to print without a heated bed or adhesive [58].

Polyethylene Terephthalate Glycol (PETG) is a popular material for desktop 3D printing due to its combination of strength and ease of use. It has good temperature resistance and is less prone to warping than ASS. PETG also has a high level of transparency and can be printed in a range of colors. However, PETG can be more difficult to print with than PLA, as it requires a higher printing temperature and can be more sensitive to print settings [59].

Nylon is a versatile material that can be used for a variety of applications, for example creating functional parts and prototypes. It has high tensile strength, flexibility, and durability, making it suitable for printing objects that require a high level of toughness. It can also be printed with a range of properties, such as increased strength or flexibility, by adjusting print settings. Nylon can be more difficult to print with than other materials, as it requires a higher printing temperature and can warp during printing. It is also more prone to absorbing moisture from the air, which can affect print quality [60].

Thermoplastic Polyurethane (TPU) and Thermoplastic Elastomer (TPE) are flexible materials that are commonly used for printing objects that require a high level of elasticity and shock absorption. They have a soft, rubber-like texture and can be printed in a range of shore hardnesses. TPU and TPE can also be printed in a range of colors and are often used for creating phone cases, shoe soles, and other similar objects. However, TPU and TPE can be more difficult

to print with than other materials, as they require precise print settings to avoid stringing and warping [61].

2.9 Ways to decrease roughness for 3D printed parts

One of the most common problems with 3D printing is rough surfaces of the printed parts. Roughness can be caused by several factors, including layer height, print speed, nozzle size, and the material used. Fortunately, there are several ways to solve this problem.

One way to decrease roughness in 3D printed parts is by adjusting the layer height. A thinner layer height can improve the overall surface finish, but this can also increase the print time. The ideal layer height will depend on the printer and the material being used. It's important to note that reducing the layer height too much can result in other issues, such as poor adhesion between layers and a weaker part. Therefore, it's essential to find the right balance between layer height and print time [62, 63, 64]. Using a smaller nozzle can also help to reduce roughness and improve surface finish. A smaller nozzle size allows for finer detail and improved accuracy, resulting in a smoother surface finish. However, using a smaller nozzle can also increase print time, and it may not be suitable for all types of prints. Therefore, it's important to consider the pros and cons of using a smaller nozzle before making the switch[62,63,64]. Post-processing techniques can also be used to reduce the roughness of 3D printed parts. Sanding, polishing, and smoothing with solvents can all improve the surface finish of the printed part. Sanding can be done using sandpaper or a sanding sponge to smooth out any rough areas. Polishing can be done using a polishing compound or a buffing wheel to achieve a high-gloss finish. Solvents such as acetone can be used to smooth out certain types of plastics, such as ASA [62,63,64]. Adding a raft or brim to the print can also help to reduce roughness. A raft or brim can help to ensure that the part adheres to the build plate, resulting in a smoother surface finish. A raft is a base layer that is printed beneath the part, while a brim is a thin layer that is printed around the perimeter of the part. Rafts and brims can also help to prevent warping and improve adhesion between the part and the build plate [62,63,64]. Adjusting the print speed can also improve the surface finish of 3D printed parts. Lower print speeds can help to reduce the roughness and improve the overall quality of the print. However, lowering the print speed can also increase the print time, and it may not be suitable for all types of prints [62,63,64].

3 Practical Part

3.1 Objectives

The objective of this study is to investigate the impact of outer surface roughness on the performance of a small rocket with a D class engine using acetone vapor smoothing on a 3D printed part. The objective is to quantify the effect of surface roughness on drag, thrust, and stability of the rocket, and to determine the effectiveness of acetone vapor smoothing in reducing surface roughness and improving performance. The objective is also to determine the most efficient and effective method of applying acetone vapor smoothing to 3D printed rocket parts and to explore the influence of other factors such as material type and manufacturing process on the performance of the rocket. The overall goal is to improve the performance of small rockets with D class engines through the optimization of surface roughness and to provide insight into the factors that influence the performance of small rockets.

3.2 Hypothesis

H_0: Higher surface roughness causes a significance increased in drag forces and therefore a decrease in maximum reached altitude.

3.3 Materials and methods

3.3.1 3D Printing

For the purposes of this investigation, the desktop FDM 3D printer Ender-3 Pro (Creality, China) set as stated in Table 1. An enclosure was made from carton to keep the printing chamber at constant temperature [65]. The long-fiber thermoplastic filament material used in this study for model fabrication was commercially available which is advanced polylactic acid, ASA, light blue colored, 1.75 mm in diameter and showed ±0.05 mm tolerance from (C-Tech, Brno, Czech Republic) . It was selected because of its sensitivity to acetone surface treatment.

Filament Material	ASA
Color	Blue
AM process	FDM
Layer Height	0.2mm
infill Density	100%
Nozzle Diameter	0.4mm
Nozzle Temperature	260 C
Printing Speed	40 mm/s
Extrusion layer width	0.45
Bed Temperature	105 C
Room Temp	24C +-1

Table 1 - Printing Parameters.

3.3.2 Samples

The 3D model of the samples was created using Inventor software [67], and then exported to Cura Slicer software [68] to generate the G-code for the printer. All the samples were printed at the same time under the same conditions, there were 3 control samples and 3 samples that were treated with acetone.

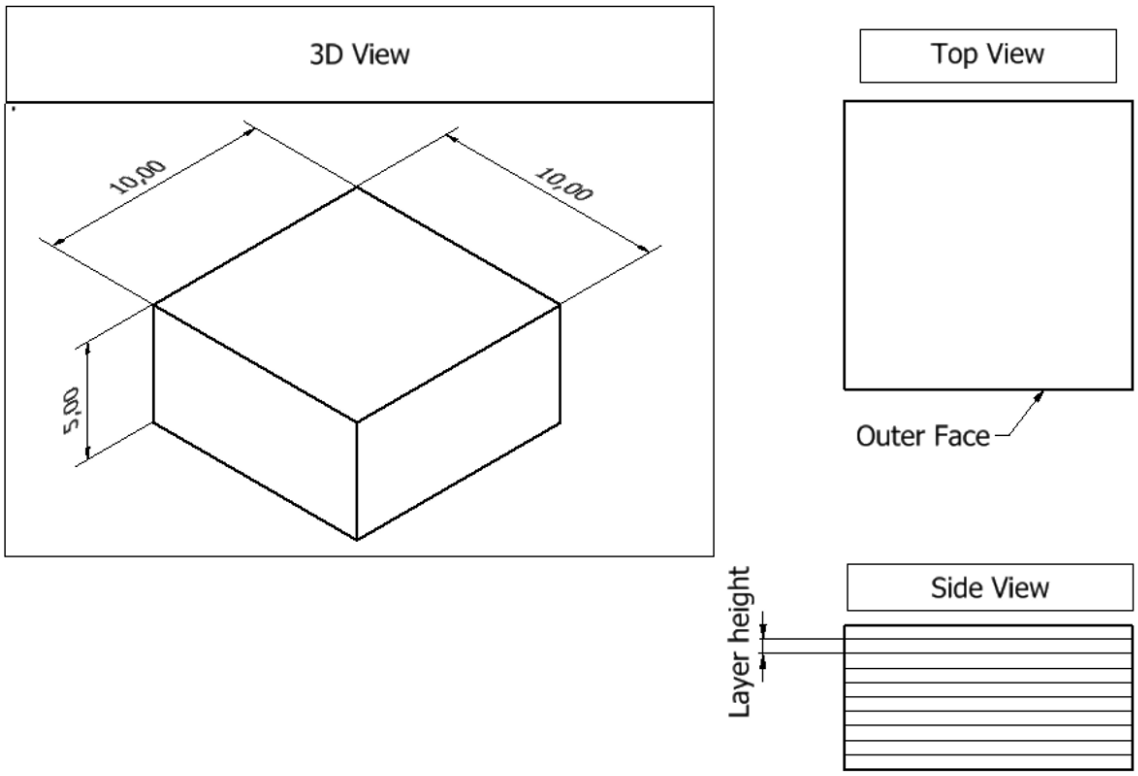

Figure 24 - Proposed framework of the 100% infill density with inner and outer faces.

Before the samples were put in the confocal microscope, they were glued to a glass platform to secure minimum movement while acquiring the images.

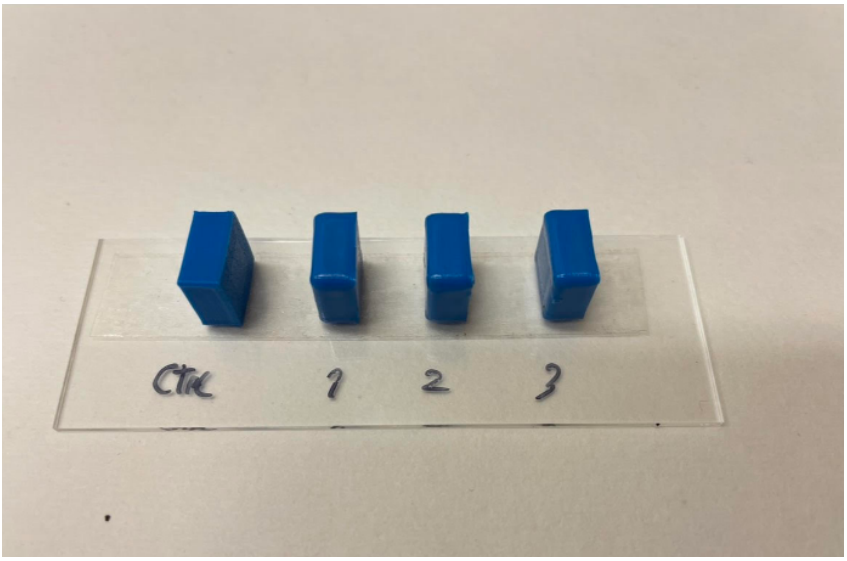

Figure 25 - Samples before being analyzed by the microscope.

3.3.3 Surface treatment method

Using the method for Acetone vapor polishing explained in Chapter 2.5 (Acetone vapor polishing) the process followed was:

- Prepared the acetone bath: A PET (Polyethylene terephthalate) plastic container was used because it's not reactive to acetone and its transparent, a small fan was added to circulate the air inside.

- Preheated the part: Before exposing the part to the acetone vapor, it was preheated to enhance the smoothing effect.

- Placed the part in the acetone bath: Making sure that the part does not touch the acetone, as this would result in dissolving the plastic rather than smoothing it.

- Sealed the container: Closed the lid of the container securely to create a vapor-tight seal.

- Wait for the smoothing effect to occur: Allowed the part to sit in the acetone vapor environment for 20 minutes.

- Removed the part from the container: After the desired time had elapsed, removed the part from the acetone bath and it was cooled to room temperature.

Figure 26 - Plastic PET container with an ASA rocket being treated with acetone vapor.

All the proper safety precautions when working with acetone were followed, such as wearing gloves and a respirator, as acetone is flammable and can cause respiratory irritation.

3.3.4 Confocal microscopy

In this bachelor's thesis the microscope used was Leica SPE (Leica Microsystems, Germany). The SPE is designed for high-resolution imaging and analysis of biological and material samples. It is equipped with a laser-based confocal scanning system that allows for high-resolution optical sectioning.

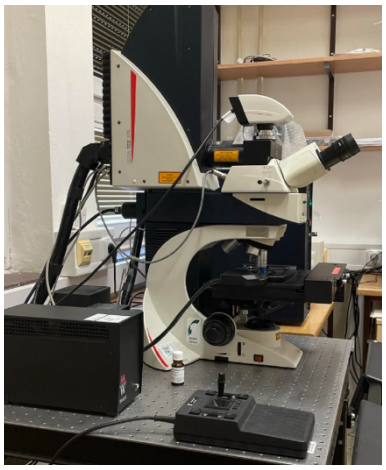

Figure 27 - Leica SPE

The SPE can capture high-resolution, three-dimensional images of samples by scanning a focused laser beam across the surface and collecting the fluorescent or reflected light. In case of detecting reflected light, the technique is called reflectance confocal microscopy (RCM). For RCM the sample is scanned at certain wavelength and the same wavelength is detected after the pinhole with a photomultiplier (PMT) detector. The sample topography is reconstructed as the laser beam is scanned over the surface. This allows analysis of surface roughness as well as other surface features such as contours, cracks and voids. SPE can be used in a variety of applications, including materials science, biology and engineering.

3.3.5 Measurement of Surface

To perform the measurement, the samples were placed under the microscope and scanned by a laser beam at 550 nm wavelength using a 10x dry objective. The scanned was perform in xz direction, i.e., the sample was scanned in x horizontal direction for 400 μm and in z vertical direction for 400 μm. The reflection of the laser beam from the sample passes through a confocal pinhole (1 Airy) and the signal is captured by a PMT detector set to 515 to 555 nm. Three samples from each group were scanned at three randomly selected places to have 9 independent measurements.

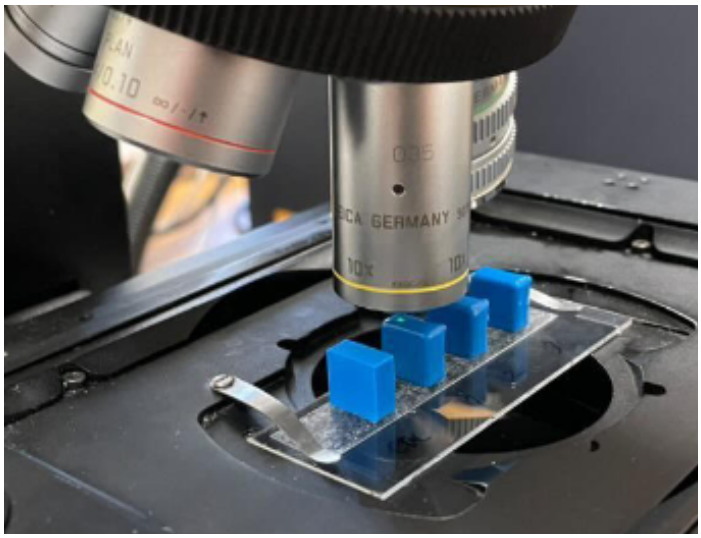

Figure 28 - Samples being scanned by the microscope.

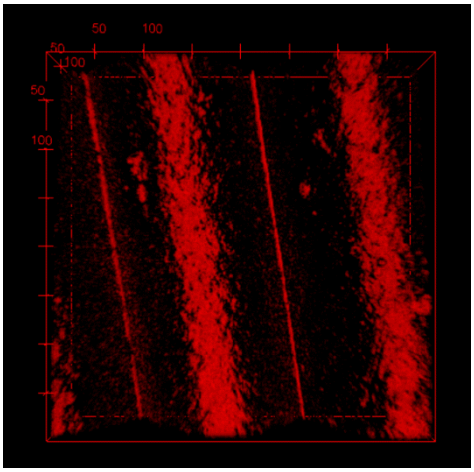

Figure 29 – 3d Image generated from the Hyperstack in Fiji.

The top-view maximum projection of the surface profile obtained from a confocal microscope Figure 29. The images were later open in Fiji image processing software as a grayscale image with metadata to obtain the data points of height variation of the sample surface. The profile was created as the intersection of the real surface and the given plane using Fiji [69]. A plane perpendicular to a plane parallel to the real surface in the appropriate direction was chosen, and then exported to excel to calculate the mean arithmetic deviation of the profile Ra.

3.3.6 Roughness computation

The median line was found using Excel function (=RANK.AVG(A2,A2:AN+1,1)/N) this calculates cumulative distribution function (CDF) where "A2" is the first data point and "N" is the total number of data points. This formula calculates the rank of the first data point relative to the entire data set, then the formula "=2*(B2-0.5)" was used, where "B2" is the first CDF value. This formula scales the CDF values to the range -1 to 1, with 0 corresponding to the median line. For each profile and after that the absolute differences between each profile height and the median line, sum the absolute differences obtained and divided the sum obtained by the number of sample points used in the roughness profile (Equation 8).

$$Ra = \frac{1}{l}\int_0^l |z(x) - z_c| dx \tag{8}$$

3.3.7 Simulation using the obtained Surface Roughness

OpenRocket is a free software for designing and simulating model rockets [66]. It was used to estimate the apogee of a rocket by inputting the relevant parameters such as mass, thrust, and surface roughness.

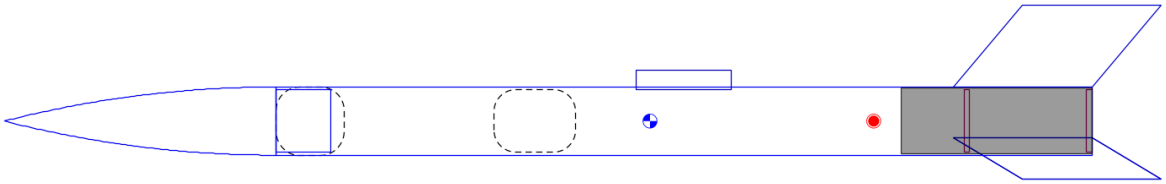

Figure 30 - Rocket simulated in OpenRocket.

Nose cone Shape	Ogive
External Diameter	25 mm
Fins shape	Trapezoidal
Number of Fins	3
Total rocket length	425 mm
Mass with motor	97.7 g
Stability	2.32 cal

Table 2 - Rocket Parameters.

4 Results of acquired roughness and simulations

The surface profile from the reflectance confocal microscopy was returned at the length of 400 um.

In the first image (Figure 31) with the rough surface profile, peaks and valleys of the surface are very pronounced and irregular. This means that the surface is highly textured and will likely have a high Ra value.

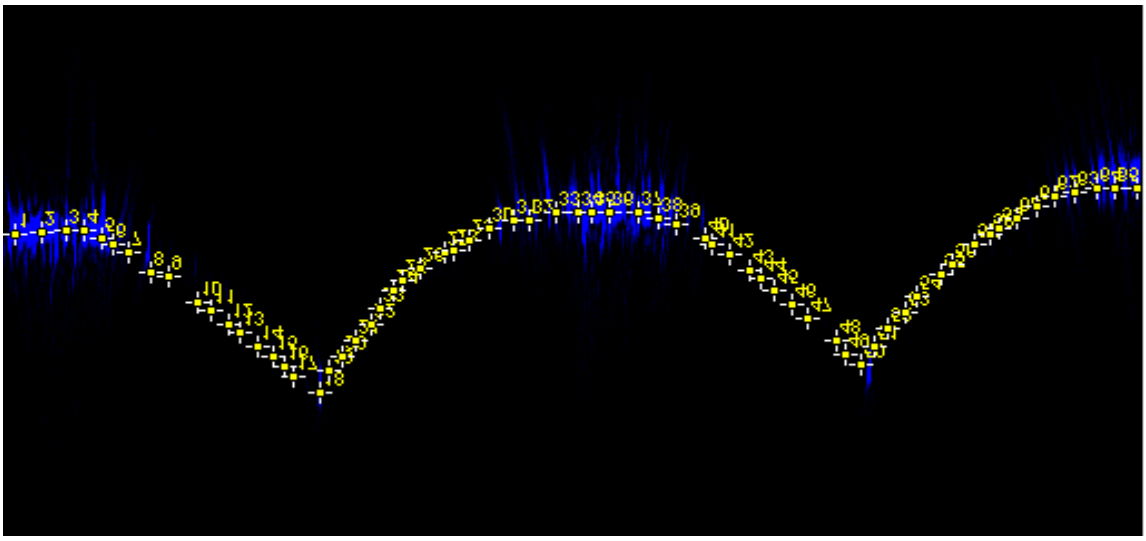

Figure 31 - Points created from the control sample profile

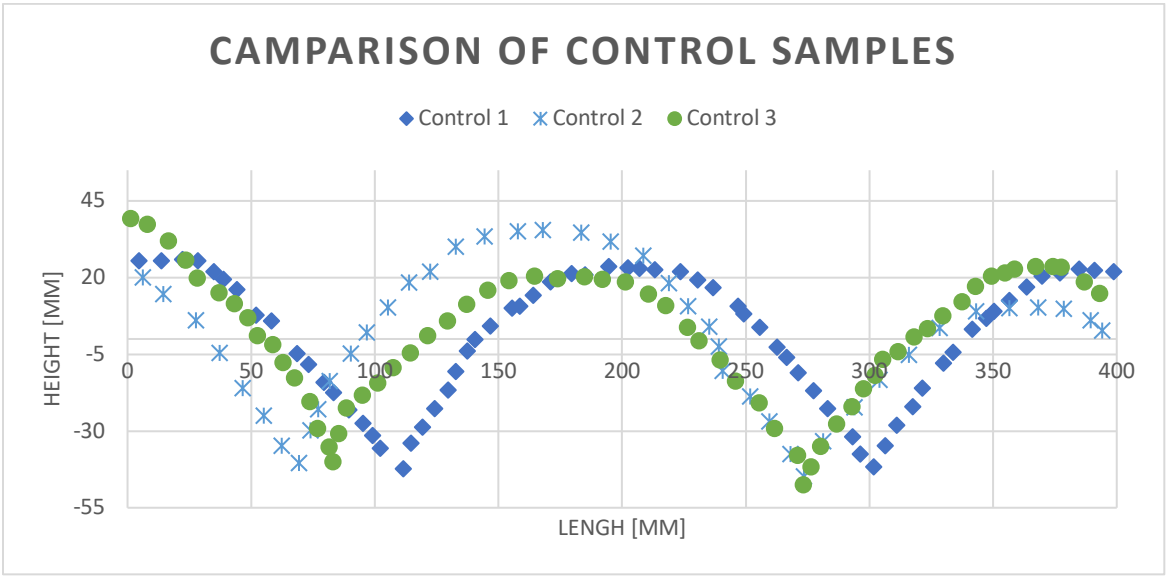

Figure 32 - Comparison of control samples profiles in excel.

In the second image (Figure 32), it can be observed that surface has been improved and appears to be much smoother than the first image. The peaks and valleys are still present, but they are much smaller and more uniform in size. This means that the surface has a lower Ra value than the first image.

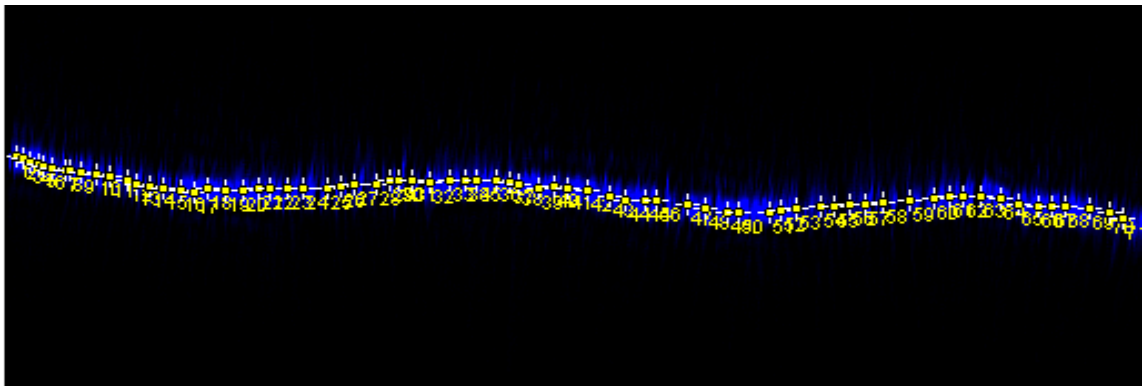

Figure 33 - Points created from the treated sample profile.

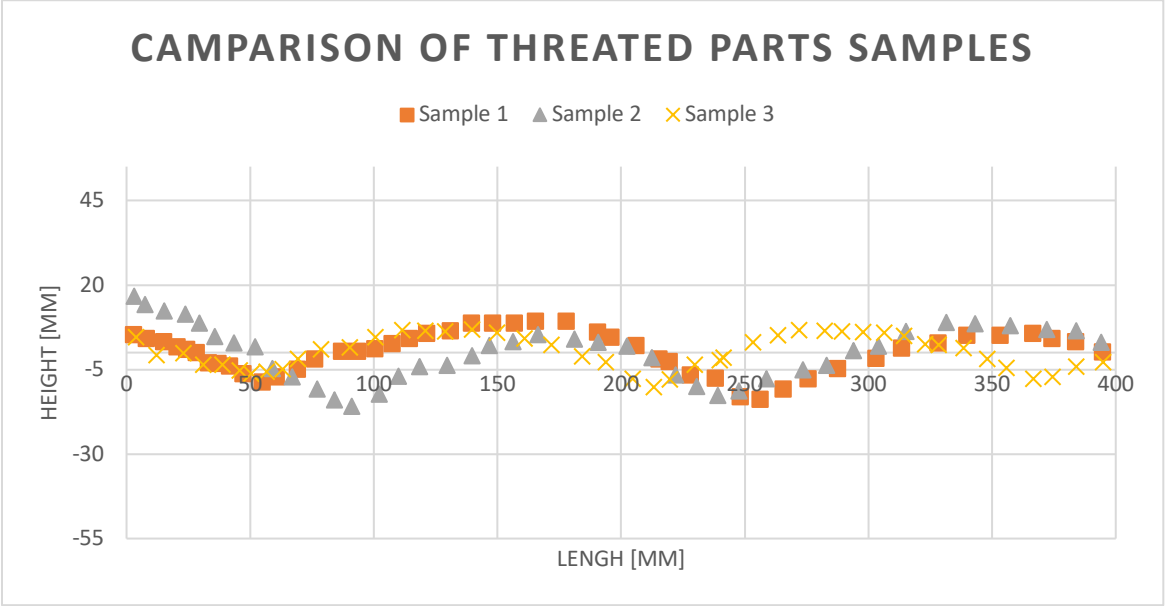

Figure 34 - Comparison of treated samples profiles in excel.

Untreated Parts					
Nozzle diameter = 0.4mm and Layer height = 0.2 mm					
Printed Part number	Measured Roughness Sample 1 (Ra)	Measured Roughness Sample 2 (Ra)	Measured Roughness Sample 3 (Ra)	Mean (Ra)	SD
1	18.70	18.88	16.96	18.18	1.06
2	22.42	23.05	18.02	21.17	2.74
3	20.52	22.69	19.32	20.84	1.71
			Average	20.06	
Treated parts					
Nozzle diameter = 0.4mm and Layer height = 0.2 mm					
Printed Part number	Measured Roughness Sample 1 (Ra)	Measured Roughness Sample 2 (Ra)	Measured Roughness Sample 3 (Ra)	Mean (Ra)	SD
1	4.49	4.88	3.05	4.14	0.96
2	4.34	6.80	6.08	5.74	1.27
3	2.65	4.41	6.53	4.53	1.94
			Average	4.81	

Table 3 - Results table

A t-test was done with the data in excel setting the significance level to 0.05 and the hypothesis to 0.

	Non threated	*Threated*
Mean	20.062	4.803
Variance	4.900	2.098
Observations	9.000	9.000
Pearson Correlation	0.185	
Hypothesized Mean Difference	0.000	
df	8.000	
t Stat	18.987	
P(T<=t) one-tail	3.06E-08	
t Critical one-tail	1.860	

Table 4 – T-Test

And the result of P one-tail is 3.06E-8 which is lower than the significance level chosen (0.05) this show that the difference between the two means is statistically significant, providing evidence to conclude that the two mean values are different, and the null hypothesis is rejected. These results were plugged into OpenRocket Software and the following simulation were obtained.

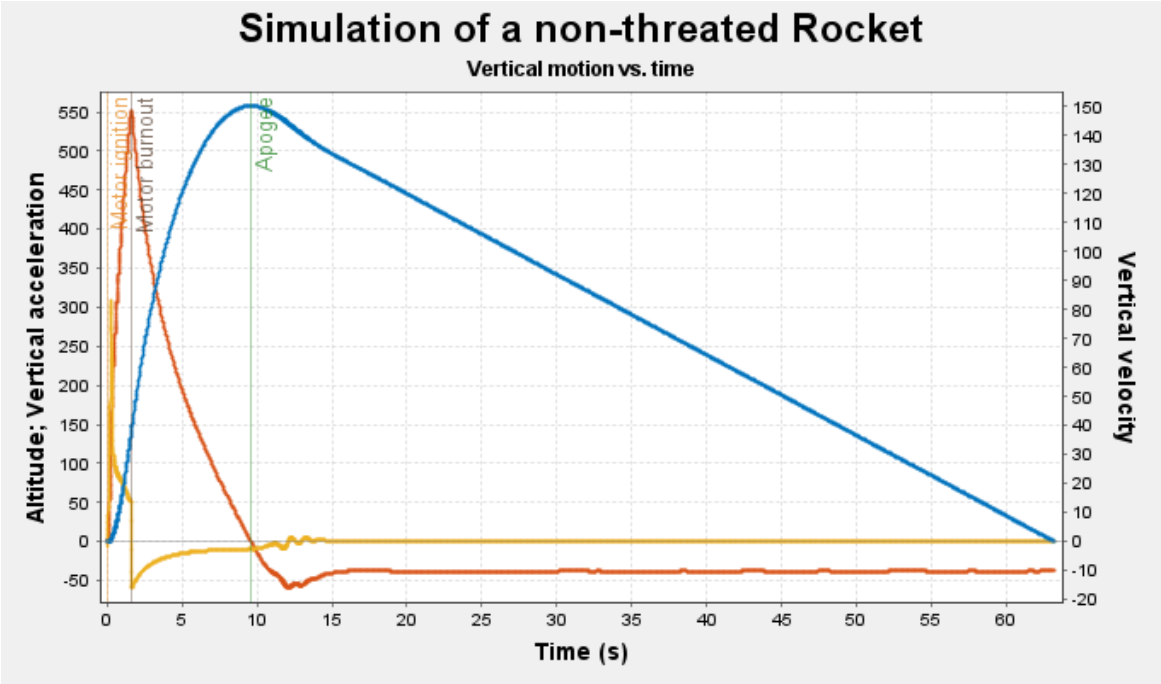

Figure 35 - Simulation of non-treated rocket

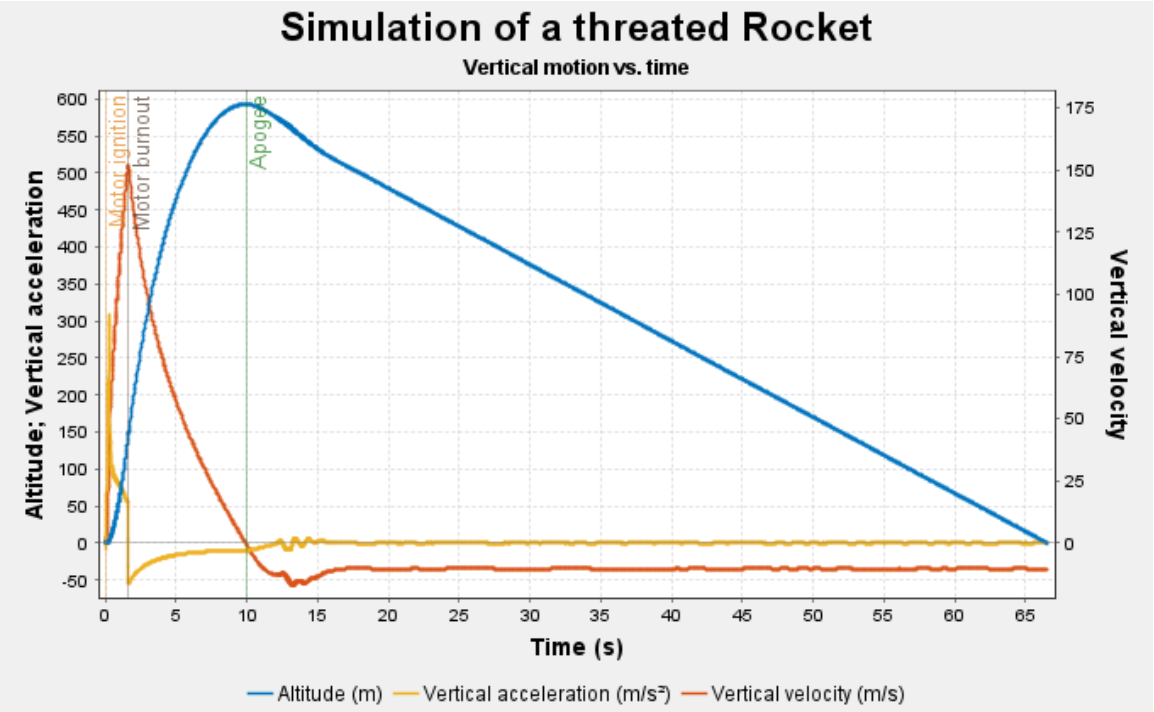

Figure 36 - Simulation of treated rocket

After the simulation of the control rocket, we can observe that the apogee of 557.8 meters is reached at 9.616 seconds. With a maximum vertical velocity of 148.614 m/s. And after the simulation of the threated rocket, we can observe that the apogee of 592.8 meters was reached at 9.93 seconds, with a maximum vertical velocity of 151.821 m/s.

5 Discussion

Comparing the results leads us to see an improvement in height of 6.27%, and an increase of vertical speed of 2.16% which is in accordance with multiple studies showing a 10% improvement in height. [23].

Based on the results it is evident that the outer surface roughness can have significant impact on the performance of small rockets with D class engines. In more detail the impact is a strong and consistent negative correlation with both the maximum altitude achieved and the maximum vertical velocity of the rocket. It was observed that rockets with smoother outer surfaces consistently achieved higher altitudes and had more maximum vertical velocity, while rockets with rougher outer surfaces tended to experience more turbulence and lower maximum vertical velocity.

To improve the roughness of the outer surfaces of the rockets in this bachelor's thesis, I used a method involving acetone vapor. This method involves exposing the rocket to acetone vapor, which can effectively melt and smooth out any rough spots or imperfections on the surface of the rocket. In average the surface roughness was improved from Ra 20.06 to Ra 4.81 which is an approximate 76% improvement in roughness other studies achieved around 90% at best, this shows that this bachelor's thesis is in accordance with other studies when it comes to reducing the surface roughness [80].

These findings have important implications for the field of rocketry and engineering. They suggest that acetone vapor treatment may be a useful tool for improving the performance of rockets, particularly those with D class engines. By using this method, manufacturers may be able to minimize surface roughness and improve the overall flight characteristics of their rockets, leading to better performance and greater reliability.

At the same time, it's important to note that the use of acetone vapor may not be suitable for all rocket designs or materials, and further research is needed to determine its efficacy in other contexts. Nonetheless, these results demonstrate the potential benefits of this method for improving rocket performance and suggest that it may be a valuable tool for engineers and manufacturers to consider in their design and manufacturing processes.

6 Conclusion

The study aimed to understand the impact of outer surface roughness on the performance of a small rocket with a D class engine. Through thorough research and experimentation, it was found that surface roughness can significantly affect the aerodynamics of a small rocket, leading to increased drag and decreased performance. The use of acetone vapor smoothing on a 3D printed part was found to be an effective method for reducing surface roughness and improving performance. However, it is important to realize that the change of dimensions of the parts that were treated with acetone vapor was not considered.

It is important to note that the findings of this study have implications for the design and production of small rockets, particularly in the field of hobby rocketry and amateur rocketry. The results highlight the importance of considering surface roughness when designing and manufacturing small rockets, and the potential benefits of using acetone vapor smoothing to improve performance.

In future research, it would be valuable to explore the impact of surface roughness on other aspects of small rocket performance, such as stability and durability, as well as to examine the effectiveness of other methods for reducing surface roughness. Overall, the findings of this thesis demonstrate the significant impact that surface roughness can have on the performance of a small rocket with a D class engine, and the potential for acetone vapor smoothing to improve performance.

7 References

[1] - M. L. Adams, Surface roughness measurement, 2nd ed. New York: Springer, 2011.

[2] - S. R. Agnew, "Surface Roughness Analysis and Measurement Techniques," National Institute of Standards and Technology, Technical Note 1297, 1995.

[3] - A review of surface roughness effects on tribology and lubrication, by T. Nikas and A. Matthews (2017). https://www.sciencedirect.com/science/article/pii/S0301679X17301903

[4] - Surface roughness effects on the mechanical properties of materials, by M. Hojjati and M. R. Ayatollahi (2019). https://link.springer.com/article/10.1007/s10853-019-03959-6

[5] - The effect of surface roughness on the adhesion of coatings, by S. L. Brown, et al. (2018). https://www.sciencedirect.com/science/article/pii/S0301679X18300491

[6] - Surface roughness and its role in the adhesion and interactions of cells and tissues, by L. G. Griffith and M. A. Swartz (2006).
https://www.sciencedirect.com/science/article/pii/S1369702106000212

[7] - Surface roughness optimization for biomaterials applications, by A. S. Popat, et al. (2007). https://www.sciencedirect.com/science/article/pii/S0142961206009361

[8] - ISO (1997). ISO 4287 Geometrical Product Specifications (GPS) – Surface texture: Profile method – Terms, definitions and surface texture parameters.

[9] - Machining Handbook - Book for practitioners. Prague: Scientia, s.r.o., 1997.
ISBN 91-97 22 99-4-6.

[10] - Surface roughness. Prague: SNTL, 1989.

[11] - Basics of construction. Prague: CTU, 1996.

[12] - Company - History. Blum-Novotest.de. [Online] Blum Novotest, 2016.

[13] - DAGNALL, H. Exploring surface texture. Leicester: Rank Taylor Hobson, 1980.

[14] - E. J. Carriveau, M. R. Islam, and S. Saha, "Surface roughness and its effects on the aerodynamic performance of wind turbine blades," Renewable and Sustainable Energy Reviews, vol. 25, pp. 401-419, 2013.

[15] - B. L. Smith and P. E. Cramer, "Surface roughness effects on the drag of two-dimensional bluff bodies," Journal of Fluids and Structures, vol. 21, no. 1, pp. 61-79, 2005.

[16] - S. S. Girimaji, "Flow simulations and experiments in wall-bounded flows: A perspective," Annual Review of Fluid Mechanics, vol. 49, pp. 447-476, 2017.

[18] - J. S. Suh, J. W. Lee, and K. J. Park, "A review of wind turbine aerodynamics research," International Journal of Precision Engineering and Manufacturing, vol. 15, no. 4, pp. 687-698, 2014.

[19] - H. K. Versteeg and W. Malalasekera, An introduction to computational fluid dynamics: the finite volume method, 2nd ed. Harlow: Pearson Education, 2007.

[20] - P. Chattopadhyay, A. Baidya, and A. Kumar, "Optimization of automobile aerodynamics," Journal of Mechanical Science and Technology, vol. 30, no. 1, pp. 217-235, 2016.

[21] - B. Balachandran, K. M. Pandey, and S. Saha, "Numerical optimization of surface roughness for aerodynamic drag reduction," Applied Soft Computing, vol. 84, 105736, 2019.

[22] - J. W. Lashley and C. M. Rumminger, "Effect of surface roughness on the aerodynamic performance of model rockets," Journal of Spacecraft and Rockets, vol. 49, no. 6, pp. 1085-1092, 2012.

[23] - M. S. Selig and S. G. Winograd, "Surface roughness effects on model rocket drag," Journal of Aircraft, vol. 20, no. 9, pp. 767-772, 1983.

[24] - H. Schlichting, Boundary-Layer Theory, 7th ed., Springer-Verlag, 1979.

[25] - P. Sturtevant and H. R. Jones, "The effect of surface roughness on the drag of blunt bodies," Journal of Fluid Mechanics, vol. 1, no. 2, pp. 131-144, 1956.

[26] - Rocket Aerodynamics - Sutton Program Article 5, GU Rocketry, 27 Aug 2021
https://www.rs-online.com/designspark/rocket-aerodynamics-sutton-program-article-5

[27] - ASTM International. (2016). Standard Test Method for Surface Roughness and Waviness of Textile Fibers by Stylus Method. ASTM D3888-16.

[28] - Alhaddad, A., & Katikaneni, S. P. (2016). Measurement of Surface Roughness Using Atomic Force Microscopy: A Review. Measurement Science and Technology, 27(12), 122001.

[29] - Thibault J, et al. (2016). Roughness characterization of optical surfaces. In Advances in optical metrology (pp. 311-339).

[30] - Muralikrishnan, B., & Ramkumar, J. (2017). Surface Roughness Measurement Using Confocal Microscopy - A Review. Materials Today: Proceedings, 4(1), 126-133.

[31] - Wang J, et al. (2018). Confocal microscopy: a powerful tool for characterizing rough surfaces. Tribology International, 128, 372-382.

[32] - Wikipedia. 2001. “Atomic force microscopy.” https://en.wikipedia.org/wiki/Atomic_force_microscopy

[33] - Károly Havancsák, High-Resolution Scanning Electron Microscopy. https://www.technoorg.hu/news-and-events/articles/high-resolution-scanning-electron-microscopy-1/

[34] - "Polishing of Surfaces" by H. Liebl, A. Tausend, and H. Bachmann, Wiley-VCH Verlag GmbH & Co. KGaA, 2010.

[35] - "Surface Treatment of Materials for Adhesive Bonding" by Sina Ebnesajjad, William Andrew Publishing, 2014.

[36] - "Powder Coating: A How-to Guide for Automotive, Motorcycle, Bicycle and Other Parts" by Jeff Zurschmeide, CarTech Inc., 2019.

[37] - "Surface Modification of Polymers: Chemical, Biological and Surface Analytical Methods" edited by S. P. Singh and J. H. Xin, Springer, 2016.

[38] - "Plastics Surface and Finish: A Global Guide to the Technology of Surface Finishing of Plastics" by Brydson and Gilbert, William Andrew Publishing, 2011.

[39] - "Electropolishing of Metals and Alloys" by Andrej M. Kritschewsky and Peter J. Gellings, Elsevier, 1990.

[40] - "Plasma Surface Modification of Polymers: Relevance to Adhesion" edited by Michael J. Owen and Kash L. Mittal, Wiley, 2013.

[41] - "Laser Surface Engineering: Processes and Applications" edited by Jonathan Lawrence and Andrew J. Pinkerton, Woodhead Publishing, 2015.

[42] - Gibson, I., Rosen, D. W., & Stucker, B. (2014). Additive manufacturing technologies: 3D printing, rapid prototyping, and direct digital manufacturing.

[43] - Wohlers, T. (2020). Wohlers Report 2020: 3D printing and additive manufacturing state of the industry annual worldwide progress report. Wohlers Associates, Inc.

[44] - Attaran, M. (2017). The rise of 3-D printing: The advantages of additive manufacturing over traditional manufacturing. Business Horizons.

[45] - Guo, N., & Leu, M. C. (2013). Additive manufacturing: technology, applications and research needs. Frontiers of Mechanical Engineering, 8(3), 215-243.

[46] - Rosen, D. W. (2017). Additive manufacturing: opportunities and challenges. Assembly Automation, 37(1), 1-3.

[47] - Berman, B. (2012). 3-D printing: The new industrial revolution. Business Horizons, 55(2), 155-162.

[48] - Stratasys. (2016). Vapor smoothing: An alternative to finishing FDM parts. Retrieved from https://www.stratasys.com/-/media/files/support/misc/vapor-smoothing-white-paper.pdf

[49] - Bower, C., Arnold, C., and Hirsch, M. (2017). Finishing of 3D printed parts: Techniques and considerations. Additive Manufacturing, 16, 69-78.

[50] - Liu, L., Huang, S., and Hu, Y. (2019). Acetone vapor polishing of fused deposition modeling 3D-printed ABS parts: Effects of process parameters. Journal of Manufacturing Processes, 41, 163-171.

[51] - Campbell, I., Bourell, D., & Gibson, I. (2012). Additive manufacturing: rapid prototyping comes of age. Rapid Prototyping Journal, 18(4), 255-258.

[52] - Wohlers, T. (2021). Wohlers Report 2021: 3D Printing and Additive Manufacturing State of the Industry. Wohlers Associates, Inc.

[53] - Additive manufacturing at home. (2021). Science, 373(6553).

[54] - FDM 3D Printing: Desktop vs. Industrial. Available at: [https://xometry.eu/en/fdm-3d-printing-desktop-vs-industrial/]

[55] – Creality https://www.creality3dofficial.eu/ \

[56] – E-plus-3d https://www.eplus3d.com/products/sls-3d-printer/

[57] - "3D Printing of Polylactic Acid (PLA): A Review." Journal of Polymers and the Environment. https://link.springer.com/article/10.1007/s10924-017-0986-7

[58] - What is ASA Filament? Properties, Pros, and Cons." 3D Insider. https://3dinsider.com/asa-filament/

[59] - "PETG Filament – Complete Guide to 3D Printing with PETG." 3D Insider. https://3dinsider.com/petg-filament/

[60] - "Nylon Filament – Complete 3D Printing Guide." 3D Insider. https://3dinsider.com/nylon-filament/

[61] - "A Beginner's Guide to 3D Printing Flexible Filament." MatterHackers. https://www.matterhackers.com/articles/a-beginners-guide-to-3d-printing-flexible-filament

[62] - Influences of Material Selection, Infill Ratio, and Layer Height in the 3D Printing Cavity Process on the Surface Roughness of Printed Patterns and Casted Products in Investment Casting. Available at: [https://www.mdpi.com/2072-666X/14/2/395]

[63] - Sood, A.K., R.K. Ohdar, and S.S. Mahapatra, Improving dimensional accuracy of Fused Deposition Modelling processed part using grey Taguchi method. Materials & Design, 2009

[64] - Sun, Q., et al., Effect of processing conditions on the bonding quality of FDM polymer filaments. Rapid Prototyping Journal, 2008.

[65] – Ender-3 Pro. Available at: [https://www.creality.com/products/ender-3-pro-3d-printer]

[66] - https://openrocket.info/

[67] - https://www.autodesk.cz/products/inventor/overview

[68] - https://ultimaker.com/software/ultimaker-cura

[69] - https://imagej.net/software/fiji/

[70] - W.E. MOERNER, Microscopy beyond the diffraction limit using actively controlled single molecules, https://onlinelibrary.wiley.com/doi/full/10.1111/j.1365-2818.2012.03600.x

[80] - Viviane Pestano, Mariana Pohlmann, Fabio Pinto da Silva, Effect of Acetone Vapor Smoothing Process on Surface Finish and Geometric Accuracy of Fused Deposition Modeling ABS Parts. https://www.scirp.org/pdf/msce_2022102111143106.pdf